processes

MDPI

Article

Analysis of Kinetic Effects of Nanofibrillated Cellulose on MMA Polymerization via Temperature Monitoring

David Victoria-Valenzuela *, Ana Beatriz Morales-Cepeda * and Sergio Alejandro De La Garza-Tenorio

Departamento de División de Posgrado e Investigación, Tecnológico Nacional de México/Instituto Tecnológico de Ciudad Madero, Parque Tecnia (Pequeña Y Mediana Industria), Bahía Aldahir, Altamira 89603, Tamaulipas, Mexico; g15071607@cdmadero.tecnm.mx

* Correspondence: david.vv@cdmadero.tecnm.mx (D.V.-V.); ana.mc@cdmadero.tecnm.mx (A.B.M.-C.)

Abstract

This study investigates the influence of cellulose nanofibrils (CNFs) on the polymerization kinetics of methyl methacrylate (MMA) during in situ suspension polymerization at 70 °C (343.15 K). Four CNF concentrations were evaluated and compared to a reference system without CNFs. Polymerizations were carried out in a thermostatted flask immersed in an ethylene glycol bath and covered to ensure thermal stability. The temperature profiles of both the reaction medium and the surrounding bath were continuously recorded, allowing for the calculation of heat flow, polymerization rate (R_p), and monomer conversion. The incorporation of CNFs led to a significant increase in R_p and faster MMA conversion. This effect was attributed to the presence of nanocellulose within the polymerizing medium, which restricted diffusion and contributed to the onset of the phenomenon of autoacceleration. Additionally, CNFs promoted a higher total heat release, underscoring the need for thermal control during scale-up. The resulting material qualifies as a biocomposite, as biobased nanofibrils became integrated into the polymer matrix. These findings demonstrate that CNFs act as effective kinetic promoters in MMA polymerizations and may serve as functional additives to enhance both reaction performance and sustainability. However, safety considerations remain critical when transferring this approach to industrial processes.

Keywords: fibrillated nanocellulose; suspension polymerization; methyl methacrylate; polymerization rate

check for updates

Academic Editor: Selestina Gorgieva

Received: 15 June 2025
Revised: 29 July 2025
Accepted: 31 July 2025
Published: 5 August 2025

Citation: Victoria-Valenzuela, D.; Morales-Cepeda, A.B.; De La Garza-Tenorio, S.A. Analysis of Kinetic Effects of Nanofibrillated Cellulose on MMA Polymerization via Temperature Monitoring. *Processes* **2025**, *13*, 2476. https://doi.org/10.3390/pr13082476

Copyright: © 2025 by the authors. Licensee MDPI, Basel, Switzerland. This article is an open access article distributed under the terms and conditions of the Creative Commons Attribution (CC BY) license (https://creativecommons.org/licenses/by/4.0/).

1. Introduction

While poly(methyl methacrylate) (PMMA) is a widely used material, the polymerization of methyl methacrylate (MMA) to obtain PMMA involves significant risks, particularly thermal ones. As in other exothermic reactions, proper control of heat release is crucial to prevent thermal hazards, such as uncontrolled reactions [1]. The existing literature includes studies addressing thermal safety and the kinetic mechanisms involved in MMA polymerization. For example, some studies have analyzed the effects of monomer concentrations on their exothermic behavior using calorimetric techniques [2], while others focused on challenges related to monitoring indirect measurements, including variations in parameters such as heat capacity and heat loss to the environment during polymerization [3]. Therefore, continued research into the thermal evolution of this and similar reactions is important for scaling up processes and safety considerations, both in laboratory work and industrial applications.

At the same time, increasing attention has been given to the development of PMMA composites reinforced with biobased materials such as nanocellulose, due to their potential benefits from both an environmental perspective and the improved properties of the final material. Nanocellulose—a nanoscale form of cellulose and itself a biopolymer—serves as a natural reinforcement with excellent characteristics, including high crystallinity and outstanding mechanical performance, as well as biodegradability and worldwide abundance. The incorporation of nanocellulose into the PMMA matrix can offer several advantages that meet the current needs of various industries, such as improved mechanical properties, sustainable processes, and a reduction in the environmental impacts of traditional plastics [4].

Among these advantages, enhanced strength and rigidity are frequently highlighted, which are crucial for applications requiring a balance between transparency and structural integrity. The rigidity imparted by nanocellulose is mainly associated with its high crystallinity, which contributes to the mechanical reinforcement of the polymer matrix. In addition, nanocellulose-based materials may exhibit a certain degree of transparency, a property attributed to the nanoscale dimensions of the fibrils, which minimize light scattering due to their size being smaller than the wavelength of visible light [5–8]. The incorporation of these natural reinforcements enables the production of PMMA with improved performance characteristics without relying on synthetic additives that may have adverse environmental impacts.

Additionally, the high crystallinity of nanocellulose is a characteristic that may influence its behavior during polymerization. This property, which depends on the source material and extraction method [4], could play a significant role in modulating transport phenomena within the reaction medium. It is plausible that the crystalline nature of nanocellulose contributes to diffusional restrictions by limiting molecular mobility or altering the microviscosity of the system, thereby affecting polymerization kinetics. In support of this hypothesis, nanocellulose has been observed to increase the viscosity of certain suspensions, with values ranging from low to high [4]. Although the specific impact of crystallinity cannot be conclusively isolated from other factors—such as dispersion state, aspect ratio, or surface chemistry—it remains an important consideration when evaluating the role of nanocellulose in the polymerization behavior of complex systems.

With regard to the development of nanocellulose-reinforced polymer matrices, a critical aspect to consider is the quality of nanocellulose dispersion within the reaction medium. Effective dispersion not only ensures uniform distribution of the reinforcing phase but also plays a key role in modulating the polymerization behavior and the final properties of the composite. Several studies have demonstrated that functionalization of nanocellulose, such as grafting hydroxybutyl acrylate onto CNC, can significantly enhance its compatibility and stability in organic solvents, improving dispersion and preventing coagulation or sedimentation. Other nanostructures, including carbon nanotubes and halloysite nanotubes, have also shown improved dispersion and mechanical reinforcement when combined with biopolymeric matrices like bacterial cellulose or regenerated cellulose. Additionally, nanocomposites such as CMC/graphene oxide and CA/acetylated nanowhiskers have revealed strong interactions, homogeneous morphologies, and enhanced mechanical and thermal properties. These findings highlight that tailoring the surface chemistry of nanocellulose via methods like silanization, acetylation, oxidation, or carboxymethylation is crucial for achieving stable dispersions and efficient reinforcement. Thus, dispersion behavior must be carefully considered when evaluating nanocellulose performance in polymer matrices [4,7].

However, despite these advances, most research involving nanocellulose and PMMA has focused on the evaluation of properties of the final composite, while much less is

known about the influence of nanocellulose on the thermal and kinetic behaviors of the polymerization reaction itself.

In this context, the present work is not oriented toward characterizing the mechanical or optical properties of the resulting material but, rather, toward understanding how the incorporation of CNFs affects the polymerization kinetics and thermal profile. Considering the relevance of both MMA polymerization and detailed analysis of the evolution of heat released during this reaction, along with the potential benefits derived from the incorporation of nanocellulose into this type of polymer, the main objective of this work is to compare the heat flow released during free-radical polymerization of MMA conducted in suspension, both in the absence and presence of CNFs.

The comparison extends to the estimation of key parameters related to the kinetics of the reactions studied, such as the R_p value and the evolution of monomer-to-polymer conversion throughout the process. This approach allows for the assessment of whether CNFs contribute to accelerating the polymerization reaction and altering its thermal behavior, both of which are key elements for the design of safe and efficient processes.

The obtained results aim to contribute to the field of MMA polymerization reactions in the presence of CNFs, particularly with regard to thermal monitoring—an essential factor for preventing risks such as uncontrolled reactions or dangerous overheating. At the same time, the findings offer a basis for future research focused on optimizing polymerization under more sustainable and controlled thermal conditions, rather than focusing on the performance of the final material.

2. Materials and Methods

2.1. Experimental Part

The reagents used for the in situ suspension polymerization were as follows: MMA monomer with $\leq$30 ppm of inhibitor (MEHQ) at 99% purity (Sigma-Aldrich, Steinheim, Germany), benzoyl peroxide (BPO) as an initiator (provided by a company from the Altamira industrial port, Tamaulipas, Mexico), polyvinyl alcohol (PVOH, 30,000–70,000 mol g^{-1}, 87–90% hydrolyzed; Sigma-Aldrich, Germany) as a dispersant, and pure nitrogen (N_2).

The CNFs were obtained from Performance BioFilaments, Vancouver, BC, Canada, at 5% solid, donated by the same company that provided the BPO. The company Performance BioFilaments® produces nano-fibrillated cellulose using a patented process by their company. The ethylene glycol used in the bath was of industrial grade, and the deionized water was treated in the laboratory's deionizer.

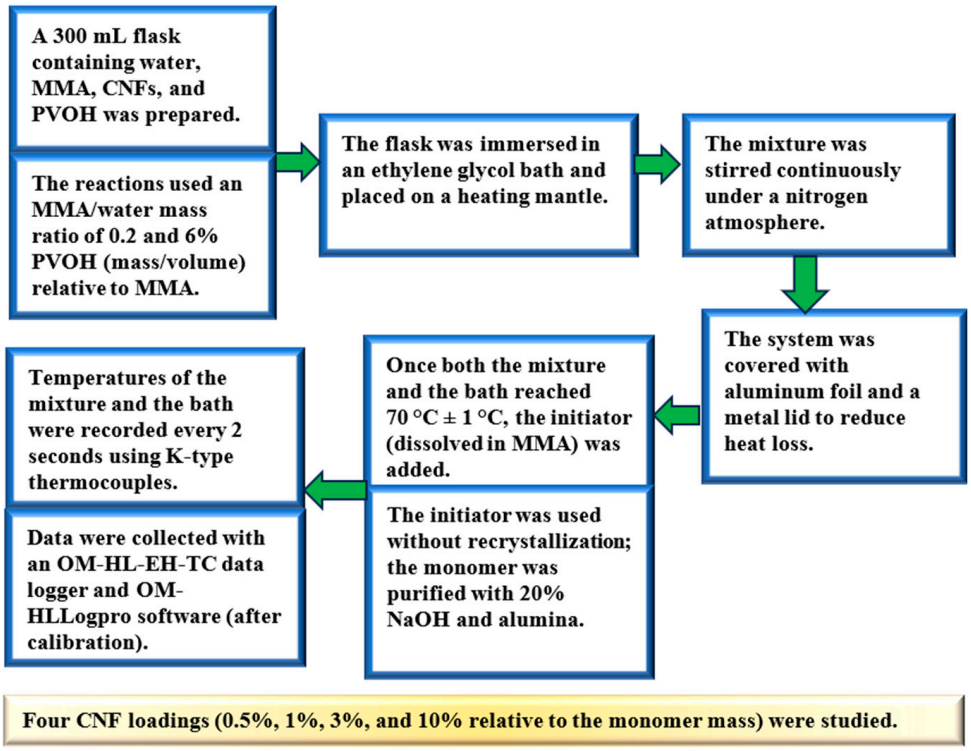
To carry out the reactions, a 300 mL flask containing a mixture of water, MMA, CNFs, and PVOH was used. This flask was immersed in an ethylene glycol bath, and the mixture was kept under constant agitation in an inert atmosphere of N_2. Both the flask and bath were placed on a heating mantle. To minimize the loss of heat to the environment, the system was covered with aluminum foil, and a metal cover was placed over the entire setup. Once both the ethylene glycol and the mixture in the flask reached a temperature of 70 °C +/− 1 °C (343.15 K +/− 1 K), the initiator (dissolved in a small amount of MMA) was added to start the reaction.

It is worth mentioning that the initiator was used without prior recrystallization, while the monomer was purified in a 20% *w*/*w* NaOH solution for 24 h. Subsequently, the monomer/NaOH solution mixture was passed through an alumina column to finally collect the purified monomer.

Each of the reactions was carried out with an MMA/water (mass/mass) ratio of 0.2, and a 6% mass/volume ratio of PVOH relative to the monomer. A total of four different amounts of CNFs were analyzed. Based on the fact that the same amount of monomer was

used in each of the reactions, amounts of 0.5, 1, 3, and 10% CNFs relative to the mass of the monomer were studied.

The temperatures of both the polymerizing mixture and the ethylene glycol were recorded every two seconds using two K-type thermocouples and a portable data logger from the OM-HL-EH-TC series by OMEGA (Norwalk, CT, USA), along with the professional software OM-HLLogpro 1.5.5 (prior calibration), which allowed us to download the necessary data for further analysis. To improve the understanding of the process, Scheme 1 presents the general experimental procedure.



Scheme 1. Schematic Diagram of the Polymerization of MMA in the Presence of CNFs.

2.2. Calculations Used in the Estimation

As the heat generated is dissipated into the medium, the heat produced by the reaction (Q_r) was estimated using an energy balance applied to the system. It was assumed that there were no heat losses to the environment and that all the heat exchanged between the mixture in the flask and the ethylene glycol bath could be calculated according to Equation (1).

$$Q_r = Q_{mix} + Q_{eg} \quad (1)$$

where Q_{mix} represents the heat flow or transfer occurring in the mixture inside the flask, and Q_{eg} corresponds to the heat flow or transfer estimated in the ethylene glycol bath. The value of Q_{mix} was calculated using Equation (2):

$$Q_{mix} = m_{MMA} c_{pMMA} \Delta T_{MIX} \Delta t^{-1} \quad (2)$$

where m_{MMA} is the mass of MMA, c_{pMMA} represents the specific heat of MMA, and ΔT_{MIX} corresponds to the change in temperature that occurred in the mixture inside the flask every two seconds (Δt). Q_{eg} is the heat flow or transfer that occurred in the ethylene glycol bath, which was estimated using Equation (3).

$$Q_{eg} = m_{eg} c_{peg} \Delta T_{eg} \Delta t^{-1} \quad (3)$$

where m_{eg} is the mass of ethylene glycol, c_{peg} is its specific heat, and ΔT_{eg} represents the change in temperature that occurred in the interval Δt.

To establish a consistent baseline for the heat flow signal, a conventional assumption was adopted; in particular, the minimum observed heat flow was considered to represent the zero-reference level. This approach is consistent with the expected behavior of an exothermic system, under the assumption that any heat flow below baseline arises from experimental noise or baseline drift rather than actual endothermic events. To reduce the influence of such noise and fluctuations, the minimum values recorded in the heat flow curves of both the reaction mixture and the ethylene glycol bath were identified. This value was then used to calculate a correction factor by adding its absolute magnitude to the entire dataset, resulting in a uniform baseline adjustment across all measurements.

With the value of Q_r, the R_p was estimated using Equation (4).

$$R_p = \frac{Q_r M_{WMMA}}{-\Delta H_p \rho_{MMA} V_{MMA}} \quad (4)$$

where M_{WMMA} is the molecular weight of MMA, ΔH_p is the theoretical heat or enthalpy of polymerization for MMA, ρ_{MMA} is the density of MMA, and V_{MMA} is the volume of MMA used.

The values used for the parameters mentioned in the previous equations are given in Table 1.

Table 1. Parameters used for calculations.

Parameter	Value	Reference
c_{pMMA}	1.791 J g^{-1} K^{-1}	[9]
c_{peg}	2.5 J g^{-1} K^{-1}	[10]
M_{WMMA}	100 g mol^{-1}	[11]
$-\Delta H_p$	57,739.2 J mol^{-1}	[12]
ρ_{MMA}	0.94 g cm^3	[13]

2.3. Characterizations

To further investigate the incorporation and structural characteristics of CNFs within the PMMA, Fourier-transform infrared spectroscopy (FTIR, Perkin Elmer Spectrum 100 FTIR spectrometer equipped with a Pike Miracle ATR accessory featuring a zinc selenide plate, manufactured in Waltham, MA, USA) and scanning electron microscopy (SEM, JSM-IT200 made in Akishima, Tokyo, Japan) were employed. FTIR analysis was used to identify functional groups associated with the chemical structures of CNFs, PMMA, and PMMA/CNFs, while SEM provided insights into the morphology and dimensions of the nanofibrils.

Sample preparation: 10 g of wet-based NFCs were added to 1 mL of isopropyl alcohol and dried at room temperature for 5 days. The sample was used for SEM and FTIR analysis. SEM and FTIR analyses of PMMA/CNFs were performed after washing and drying.

3. Results

Monitoring the temperature of the ethylene glycol revealed that, during the reaction, the heat released due to polymerization affected the system composed of both the reaction mixture and the ethylene glycol bath. This was reflected in the increases in temperature observed in both the bath and the mixture. Part of the heat generated remained in the mixture, while the rest was transferred to the ethylene glycol bath through the walls of the flask, raising the bath's temperature. Therefore, the total heat generated by the exothermic reaction is equal to the sum of the heat absorbed by the mixture and the heat absorbed by

the bath, justifying the use of Equation (1). This data trend can be attributed to the fact that the flask used for the reaction was not fully insulated, allowing some of the heat generated to escape instead of being entirely absorbed by the bath.

The temperature evolution of the suspension in which polymerization occurred for each experiment is shown in Figure 1, while the corresponding results for the ethylene glycol bath are presented in Figure 2. It can be observed that the reaction with the earliest temperature increase was the one containing the highest number of CNFs tested.

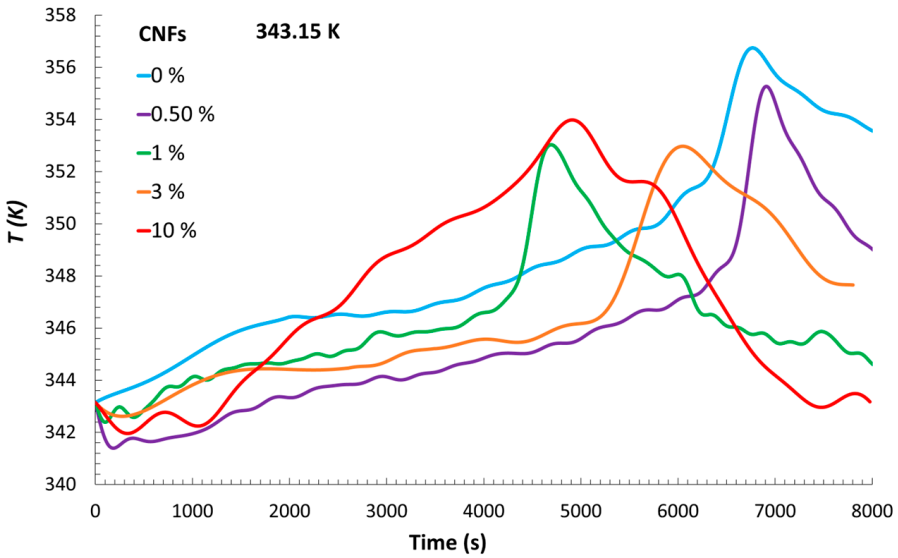


Figure 1. Evolution of the temperature in the suspension where the polymerization took place with the indicated amounts of CNFs added relative to the monomer mass.

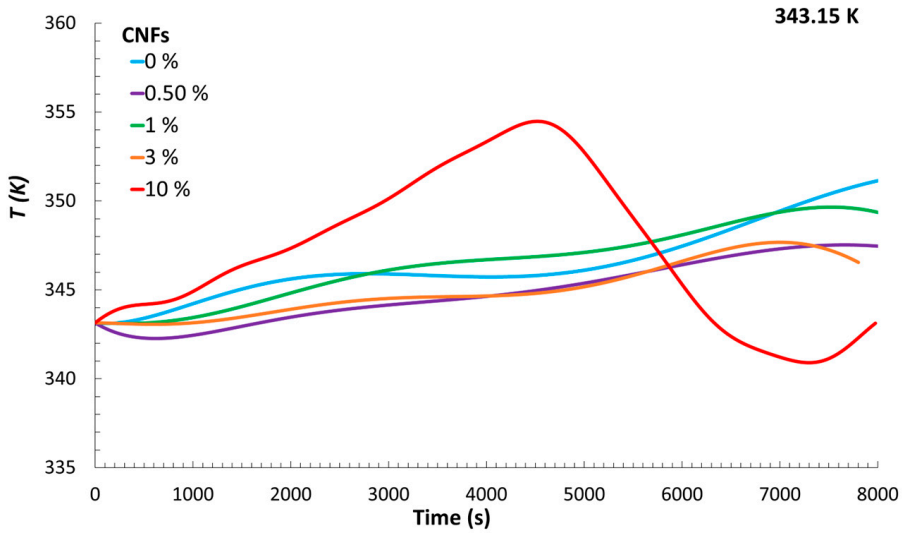


Figure 2. Evolution of the temperature in the ethylene glycol bath used in the polymerization with the indicated amounts of CNFs added relative to the monomer mass.

The heat flows corresponding to the reaction in each of the experiments are shown in Figure 3, from which a trend can be observed. Although the experiments with 0.5% CNFs and no CNFs exhibited similar heat flows, it can be seen that, with a higher content of CNFs, the maximum released heat flow increased. Consequently, the R_p values showed a similar trend (Figure 4).

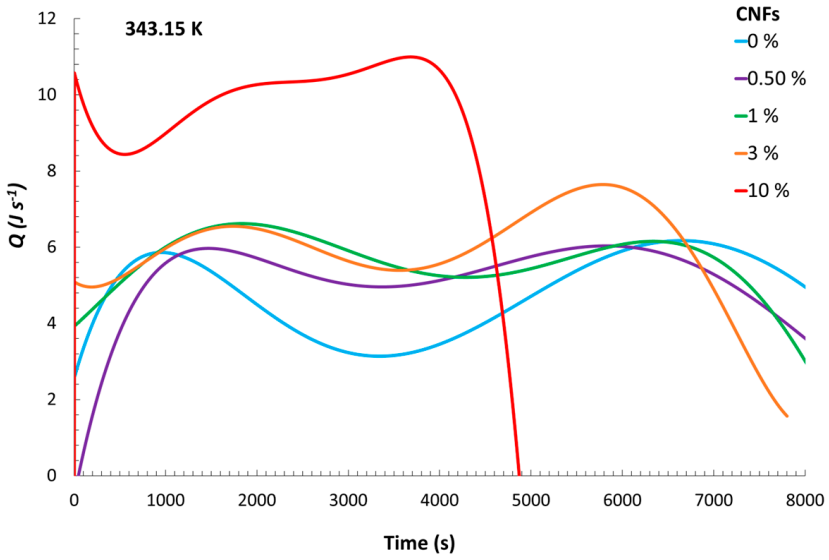


Figure 3. Evolution of the heat flow released during polymerization with the indicated amounts of CNFs added relative to the monomer mass.

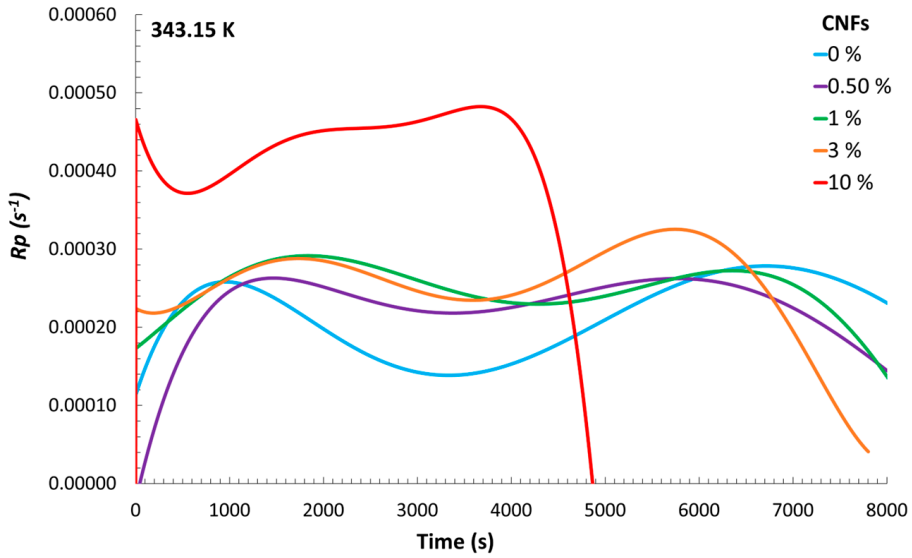


Figure 4. Evolution of the R_p values during polymerization with the indicated amounts of CNFs added relative to the monomer mass.

The monomer-to-polymer conversion evolution curves (presented in Figure 5) were obtained by integrating the R_p curves shown in Figure 4. These curves showed the same trends as those observed in the previous ones: although curves associated with similar amounts of nanocellulose tended to overlap, it can be noted that, as the reactions progressed, a higher amount of CNFs led to a faster monomer-to-polymer conversion.

With these results, it is possible to identify a relevant thermal interplay between the reaction medium and the surrounding ethylene glycol bath. The exothermic nature of the polymerization reaction resulted in the generation of heat that was not entirely retained within the reacting mixture but partially transferred through the flask walls to the external bath. This highlights the dual absorption of heat by both the reaction mixture and the ethylene glycol bath, which together account for the total heat released. The fact that the reaction vessel was not completely insulated likely contributed to this behavior, allowing a portion of the thermal energy to dissipate into the surroundings. Notably, the heat flow profiles indicated that the system containing the highest CNF concentration exhibited the most rapid increase, pointing to a more intense initial exothermic response.

This phenomenon could be attributed to increased viscosity and particle density at high CNF loadings, which may enhance reaction kinetics through diffusion-limited effects and localized concentration gradients. As a result, accelerated radical propagation or reduced heat dispersion may occur, leading to earlier temperature rises and higher peak heat flows. These coupled thermal and kinetic behaviors support the observed trends in R_p and conversion, suggesting that CNF content significantly influences not only the structural characteristics of the resulting material but also the thermodynamic evolution of the polymerization process.

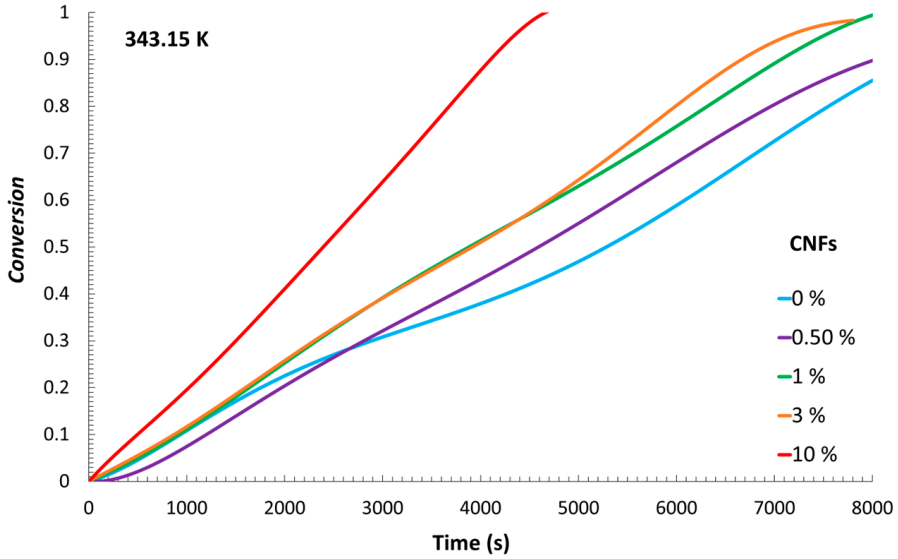


Figure 5. Evolution of the monomer-to-polymer conversion during polymerization with the indicated amounts of CNFs added relative to the monomer mass.

An interesting aspect to observe is the contrasting thermal behavior between the polymerization reactions containing 1% and 3% CNFs. The formulation with 1% CNFs exhibited an earlier rise in temperature; however, the total heat released was lower than in the 3% reaction. This phenomenon could potentially be attributed to the combined influence of CNF concentration on thermal transport and polymerization kinetics. At lower concentrations, the reaction medium may exhibit reduced viscosity and fewer diffusional constraints, facilitating faster heat dissipation and resulting in a more immediate but less intense thermal response. Conversely, the presence of 3% CNFs may lead to higher cumulative heat release, possibly due to increased monomer conversion promoted by localized viscosity increases and diffusional limitations, which in turn could enhance autoacceleration. These results suggest that CNF content may exert a complex influence on both the thermal and kinetic profiles of the polymerization process, although further investigation is needed to confirm and quantify these effects.

A particularly notable case emerges in the experiment conducted with 10% CNFs, an unusually high concentration. Under this condition, the heat flow profile displays a steep initial increase, indicative of a highly exothermic onset. However, this is followed by a sharp and premature decline in heat flow compared to the other reactions. This behavior may indicate that while elevated CNF content initially accelerates the polymerization—possibly due to extreme local viscosity or severely restricted diffusion—it might also provoke early termination or self-limiting mechanisms within the reaction medium. These observations highlight the potential trade-offs associated with excessive filler loading and reinforce the importance of optimizing CNF concentration to balance reactivity and thermal control.

The FTIR spectra for pure CNFs, pure PMMA, and PMMA/CNFs are presented in Figure 6.

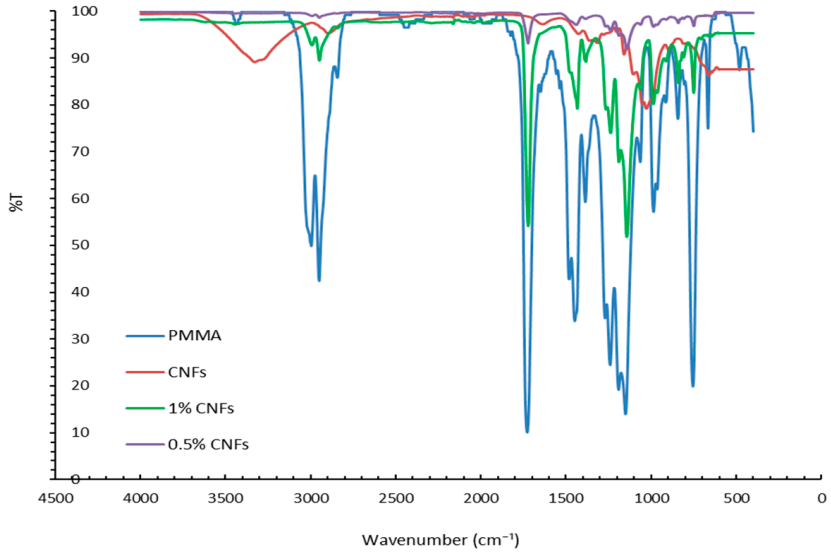


Figure 6. FTIR spectra of pure CNFs, PMMA, and PMMA/CNFs.

The spectrum of pure CNFs exhibited characteristic bands consistent with those reported in the literature for unmodified cellulose. Broad O–H stretching vibrations were identified in the ~3330–3400 cm^{-1} region, along with aliphatic C–H stretching near 2890 cm^{-1} [14,15]. Additionally, intense bands between 1200 and 1000 cm^{-1} were observed, corresponding to C–O–C and C–O vibrational modes of the glucopyranose ring. The peak at ~896 cm^{-1} was identified as a diagnostic signal of the β(1→4)-glycosidic linkage, confirming the presence of cellulose in its nanofibrillated form [14,15].

Similarly, the spectrum of pure PMMA (0% CNFs) displayed the typical bands of this synthetic polymer. A strong carbonyl (C=O) stretching vibration was observed at 1727 cm^{-1}, attributed to the ester group, along with C–H vibrations in the 2996–2950 cm^{-1} range [16,17]. The bands between 1272 and 1152 cm^{-1} were assigned to C–O–C stretching of the ester group, while the signal at ~750 cm^{-1} was associated with C–C skeletal vibrations of the polymer [16].

The spectra of the samples containing 0.5% and 1% CNFs showed a combination of signals from both PMMA and cellulose. In the 0.5% CNF sample, while the bands were similar to those of pure PMMA, additional signals at 986 and 841 cm^{-1} were also observed, which may be associated with C–O vibrations and a possible shift in the β-glycosidic peak of CNFs [14]. These signals were more pronounced in the 1% CNF sample, where the relative intensity of the C–O–C-related bands increased, and the ~841 cm^{-1} peak became more defined. Nonetheless, in both samples, the carbonyl (C=O) peak remained visible, indicating that the incorporation of CNFs did not significantly interfere with the chemical structure of PMMA [16].

Overall, these results confirm that the spectra of the PMMA/CNFs samples retain the characteristic bands of PMMA, while the incorporation of CNFs is evidenced by additional peaks in regions typical of glucopyranose-related vibrations. The intensities of these signals correlate with the CNF content in the matrix, suggesting effective incorporation of the cellulose phase even at low percentages.

Furthermore, the SEM analysis (Figures 7 and 8a,b, visualized at magnifications of ×3300 and ×170, respectively) revealed a bouquet-like structure composed of cellulose fibers with an overall average diameter of 2.268 ± 0.15 µm. This cluster is formed of individual fibers with an average diameter of 651.4 ± 8 nm and an average length of 675.5 ± 0.25 µm (Figure 8b), resulting in a length-to-diameter ratio (L/D) of approximately 1036.99. A similar L/D ratio was reported by Jian et al. (2023) [18] for holocellulose nanofibrils (L/D = 1464).

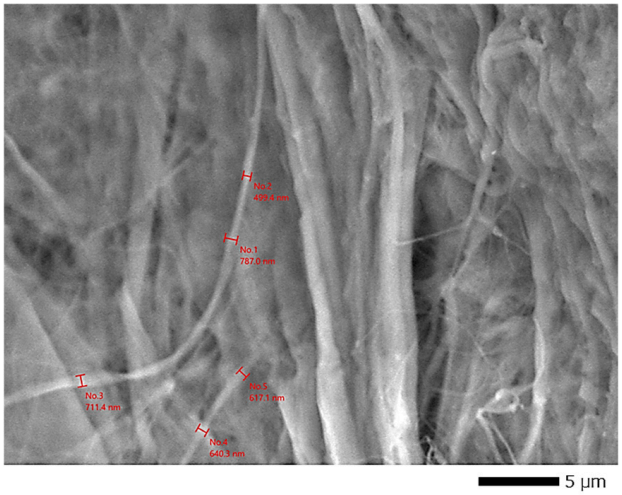


Figure 7. SEM image of CNFs observed at 3300× magnification under low-vacuum conditions, showing a bouquet-like structure composed of cellulose fibers. Measurements: diameters.

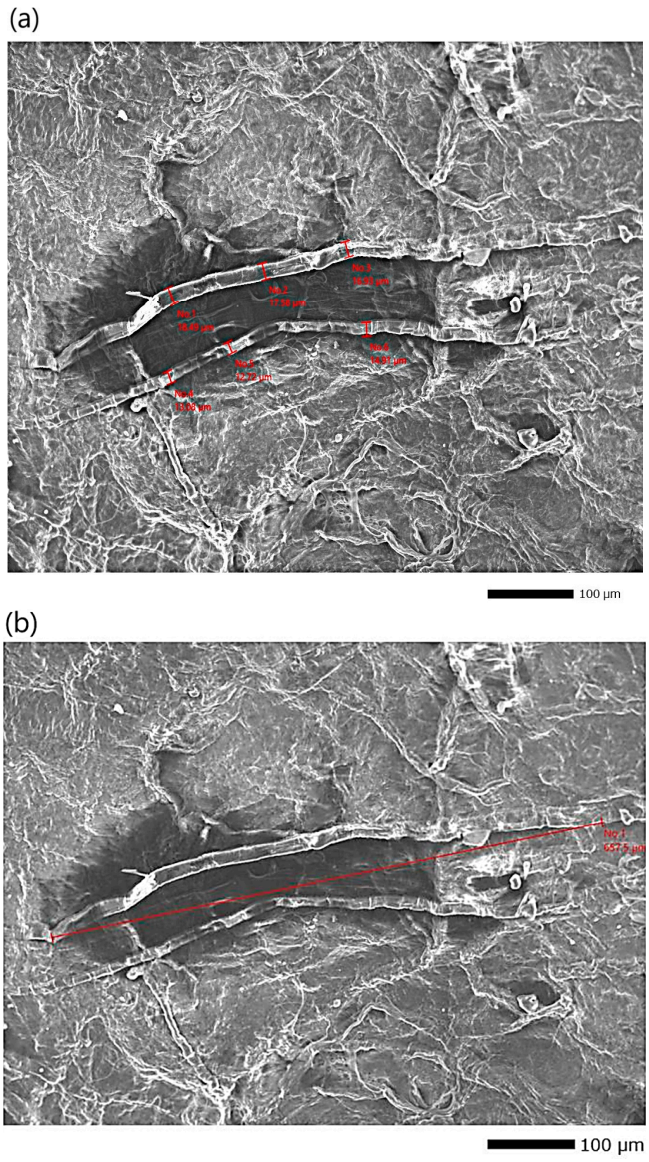


Figure 8. SEM images of cellulose CNFs at 170× magnification under high-vacuum conditions. Measurements: (**a**) diameters, (**b**) length.

4. Discussion

The results obtained in this study allow for a deeper understanding of the thermal and kinetic behaviors of the polymerization system in the presence of CNFs. Based on the data, it can be confirmed that the heat generated during the polymerization reaction was distributed between the reaction mixture and the ethylene glycol bath, providing evidence for an increase in temperature in both components. This behavior supports the hypothesis that the total heat generated corresponds to the sum of the heat absorbed by the mixture and the heat absorbed by the bath.

A key observation is that there was a clear increase in the maximum heat flow released as the concentration of CNFs in the mixture increased, which confirms that CNFs influence the amount of heat generated during the reaction. The polymerization rate (R_p) exhibited a similar trend to that of the heat flow, with higher CNF concentrations accelerating both the heat release and the reaction rate. Furthermore, integration of the reaction rate curves demonstrated that, with higher CNF content, monomer-to-polymer conversion occurred more rapidly.

These findings are consistent with and reinforce the trends previously reported by our research group, where we analyzed the evolution of monomer conversion through gravimetric measurements during polymerization in the presence of tempo-oxidized nanofibers (Victoria-Valenzuela et al., 2023 [19]). In that study, the increased polymerization rate was attributed to diffusion restrictions induced by the nanocellulose during the polymerization process, which aligns well with the thermal behaviors observed in the current work.

Additionally, it is important to consider that the increase in CNF concentration not only affects the generation of heat and the reaction rate, but may also influence the viscosity of the reaction medium. As the viscosity increases, the mobility of the macroradicals decreases, which can hinder termination reactions and thus favor the propagation step. This phenomenon is closely associated with the well-known Trommsdorff or gel effect (also referred to as the autoacceleration effect), in which a reduction in termination rate due to increased viscosity leads to a rapid increase in reaction rate and molecular weight [20]. In this context, the presence of CNFs may contribute to or amplify this effect, acting not only as a physical barrier to diffusion but also as a factor promoting autoacceleration.

Although the scientific literature includes a significant number of papers addressing the use of CNFs as reinforcement materials in polymer matrices, it is worth highlighting that this work can be considered one of the pioneers in exploring the effects of CNFs on polymerization kinetics. While the incorporation of CNFs into polymeric systems has been explored in various contexts, their application to modify the polymerization behaviors of monomers such as MMA remains relatively underdeveloped, positioning this study as an early contribution in this emerging area.

Despite the innovative character of this approach, the discussion can be enriched by comparison with previous research that examined the effects of in situ incorporation of other reinforcements on the acceleration of polymerization. For instance, studies by Nikolaidis et al. (2011) [21] have shown that the addition of specific reinforcement materials can significantly alter the kinetic characteristics of polymerization, promoting the acceleration of the process. Such precedents suggest that the introduction of CNFs into the MMA polymerization system may result in comparable effects not only in terms of improving the final material properties, but also in favoring reaction conditions that are conducive to process scalability and control.

Regarding the heat released during the reaction, this parameter becomes particularly relevant in the context of industrial implementation. The increase in heat release observed with higher CNF concentrations implies potential risks associated with the exothermic nature of the system, especially when operated at larger scales [2,22]. Therefore, thermal

management strategies and the precise control of nanomaterial loading become critical to ensure the safety and reproducibility of processes.

5. Conclusions

The analysis of materials that accelerate the polymerization rate and increase heat release is essential for understanding polymerization processes, particularly in systems intended for scale-up, where thermal control and reaction efficiency are critical. In the synthesis of PMMA-based nanocomposites, this study demonstrated that the incorporation of nanocellulose not only accelerated the polymerization reaction but also modified the thermal behavior of the system. Higher nanocellulose concentrations led to increased polymerization rates and greater heat flow, emphasizing the importance of effective thermal control. These effects were attributed to the presence of nanocellulose within the polymerizing medium, which may have imposed diffusional restrictions and contributed to the onset of autoacceleration. This behavior could be linked to the high crystallinity of nanocellulose, which may enhance its interaction with the growing polymer chains and influence local viscosity and molecular mobility.

Furthermore, the integration of biobased nanofibrils into the polymer matrix resulted in the formation of a biocomposite, providing evidence of improved reaction kinetics while promoting the development of biobased polymeric systems. This work advanced the understanding of polymerization behavior in the presence of renewable reinforcements and contributed to future studies aimed at exploiting CNFs as functional additives to improve polymerization kinetics, material properties, and process safety. The findings reported here have significant implications for the design of more efficient, safer, and environmentally conscious polymerization systems.

Author Contributions: Conceptualization A.B.M.-C. and D.V.-V.; Formal analysis, D.V.-V., A.B.M.-C. and S.A.D.L.G.-T.; Funding acquisition, A.B.M.-C.; Investigation, D.V.-V., A.B.M.-C. and S.A.D.L.G.-T.; Methodology, D.V.-V., A.B.M.-C. and S.A.D.L.G.-T.; Project administration, D.V.-V. and A.B.M.-C.; Resources, A.B.M.-C.; Supervision, A.B.M.-C.; Validation, D.V.-V., A.B.M.-C. and S.A.D.L.G.-T.; Writing—original draft, D.V.-V. and A.B.M.-C.; Writing—review, and editing, D.V.-V. and A.B.M.-C. All authors have read and agreed to the published version of the manuscript.

Funding: This research received no external funding.

Data Availability Statement: The data that support the findings of this study are available from the corresponding authors upon reasonable request.

Acknowledgments: The authors thank the Microbiology and Organic Chemistry laboratories at the Tecnológico Nacional de México, Instituto Tecnológico de Cd. Madero, for providing facilities to carry out part of the experimental work. Sergio Alejandro De La Garza-Tenorio thanks CONAHCYT (now SECIHTI) for the master's degree scholarship No. 841903. The authors would like to thank Styropek for the donation of the CNFs and the initiator used in this work.

Conflicts of Interest: The authors declare no conflicts of interest.

References

1. Westerterp, K.R.; Molga, E.J. Safety and Runaway Prevention in Batch and Semibatch Reactors—A Review. *Chem. Eng. Res. Des.* **2006**, *84*, 543–552. [CrossRef]
2. Cui, X.; Gui, X.; Hu, J.; Liu, J.; Zhou, R.; Gong, Z.; Li, W.; Yang, Y.; Dong, Y. Thermal Safety and Overall Kinetics for Methyl Methacrylate Solution Polymerization via On-line Process Analytical Technology. *Thermochim. Acta* **2023**, *730*, 179620. [CrossRef]
3. Sreeja, E.S.; Ram, V.D. Monitoring Batch Suspension Polymerization Process Based on Calorimetric-State Estimation Technique. *Chem. Eng. Commun.* **2025**, *212*, 589–602. [CrossRef]

4. Norizan, M.N.; Shazleen, S.S.; Alias, A.H.; Sabaruddin, F.A.; Asyraf, M.R.M.; Zainudin, E.S.; Abdullah, N.; Samsudin, M.S.; Kamarudin, S.H.; Norrrahim, M.N.F. Nanocellulose-Based Nanocomposites for Sustainable Applications: A Review. *Nanomaterials* **2022**, *12*, 3483. [CrossRef] [PubMed]
5. Shih, Y.F.; Chou, M.Y.; Lian, H.Y.; Hsu, L.R.; Chen-Wei, S.M. Highly Transparent and Impact-Resistant PMMA Nanocomposites Reinforced by Cellulose Nanofibers of Pineapple Leaves Modified by Eco-Friendly Methods. *Express Polym. Lett.* **2018**, *12*, 844–854. [CrossRef]
6. Ray, D.; Sain, S. In Situ Processing of Cellulose Nanocomposites. *Compos. Part A Appl. Sci. Manuf.* **2016**, *83*, 19–37. [CrossRef]
7. Feldman, D. Cellulose Nanocomposites. *J. Macromol. Sci. Part A* **2015**, *52*, 322–329. [CrossRef]
8. Banerjee, M.; Sain, S.; Mukhopadhyay, A.; Sengupta, S.; Kar, T.; Ray, D. Surface Treatment of Cellulose Fibers with Methyl-methacrylate for Enhanced Properties of In Situ Polymerized PMMA/Cellulose Composites. *J. Appl. Polym. Sci.* **2014**, *131*, 1–9. [CrossRef]
9. Sheng, M.; Dan, F.; Horsch, S.; Bellair, R.; Holsinger, M.; Scholtz, T.; Weinberg, S.; Sopchik, A. Calorimetric Method to Determine Self-Accelerating Polymerization Temperature (SAPT) for Monomer Transportation Regulation: A Heat Balance Approach. *Org. Process Res. Dev.* **2019**, *23*, 750–761. [CrossRef]
10. Yue, H.; Zhao, Y.; Ma, X.; Gong, J. Ethylene Glycol: Properties, Synthesis, and Applications. *Chem. Soc. Rev.* **2012**, *41*, 4218–4244. [CrossRef] [PubMed]
11. Sigma-Aldrich. 201-297-1. Available online: https://www.sigmaaldrich.com/MX/es/search/201-297-1?focus=products&page=1&perpage=30&sort=relevance&term=201-297-1&type=egec_number (accessed on 22 December 2024).
12. Kalfas, G.; Yuan, H.; Ray, W.H. Modeling and experimental studies of aqueous suspension polymerization processes. 2. Experiments in batch reactors. *Ind. Eng. Chem. Res.* **1993**, *32*, 1831–1838. [CrossRef]
13. PubChem. Methyl Methacrylate. Available online: https://pubchem.ncbi.nlm.nih.gov/compound/Methyl-methacrylate (accessed on 22 December 2024).
14. Colom, X.; Carrillo, F. Crystallinity Changes in Lyocell and Viscose-Type Fibres by Caustic Treatment. *Eur. Polym. J.* **2002**, *38*, 2225–2230. [CrossRef]
15. Poletto, M.; Ornaghi, H.L.; Zattera, A.J. Native Cellulose: Structure, Characterization and Thermal Properties. *Materials* **2014**, *7*, 6105–6119. [CrossRef] [PubMed]
16. Silverstein, R.M.; Webster, F.X.; Kiemle, D.J. *Spectrometric Identification of Organic Compounds*, 7th ed.; Wiley: Hoboken, NJ, USA, 2005.
17. Socrates, G. *Infrared and Raman Characteristic Group Frequencies: Tables and Charts*, 3rd ed.; Wiley: Chichester, UK, 2001.
18. Jiang, Y.; Wang, X.; Meng, Z.; Zhang, M.; Wang, S.; Liu, X. Weakening Fibril-Fibril Interactions via On-Demand Regulation of Hemicellulose Phase towards Facile Disassembly of Lignocellulose Heterostructure into Approaching Native-State Elementary Fibrils. *Green Chem.* **2023**, *26*, 879–894. [CrossRef]
19. Victoria-Valenzuela, D.; Morales-Cepeda, A.B.; Cárdenas-Rangel, E.I. Toward an Understanding of the Effects of Nanocellulose During the Free-Radical Polymerization Reactions. Kinetic Aspects of Suspension-Free Radical Polymerization of Methyl Methacrylate (MMA) in the Presence and Absence of Nanocellulose. *J. Polym. Res.* **2023**, *30*, 252. [CrossRef]
20. Odian, G. *Principles of Polymerization*, 4th ed.; Wiley-Interscience: Hoboken, NJ, USA, 2004.
21. Nikolaidis, A.K.; Achilias, D.S.; Karayannidis, G.P. Synthesis and Characterization of PMMA/Organomodified Montmorillonite Nanocomposites Prepared by in Situ Bulk Polymerization. *Ind. Eng. Chem. Res.* **2011**, *50*, 571–579. [CrossRef]
22. Zhao, J.; Gui, X.; Zhang, W.; Lin, S.; Tu, Y.; Hu, J.; He, D.; Huang, X. Thermal Hazard Evaluation of Styrene-Methyl Methacrylate Bulk Copolymerization by Differential Scanning Calorimetry and Accelerating Rate Calorimetry. *Thermochim. Acta* **2021**, *706*, 179052. [CrossRef]

Disclaimer/Publisher's Note: The statements, opinions and data contained in all publications are solely those of the individual author(s) and contributor(s) and not of MDPI and/or the editor(s). MDPI and/or the editor(s) disclaim responsibility for any injury to people or property resulting from any ideas, methods, instructions or products referred to in the content.